

# **A Covalent Organic Framework/Graphene Aerogel**

## **Electrocatalyst for Enhanced Overall Water Splitting**

Zhiya Wang,<sup>a</sup> Jingfeng Li,<sup>b</sup> Shiyin Liu,<sup>a</sup> Gaofeng Shao,<sup>\*c</sup> Xiaojia Zhao<sup>\*a</sup>

<sup>1</sup> College of Chemistry and Materials Science, Hebei Normal University, Shijiazhuang, 050024, China

<sup>2</sup> Institute of Microscale Optoelectronics, Shenzhen University, Shenzhen, 518060 P.R. China

<sup>3</sup> School of Chemistry and Materials Science, Nanjing University of Information Science & Technology, Nanjing 210044, China

\* Corresponding author (gfshao@nuist.edu.cn (Shao G), xiaojia.zhao@hebtu.edu.cn (Zhao X))

## Section 1. Materials and Methods

### 1.1. Material

All solvents and reagents obtained from commercial sources were used without further purification. Graphene oxide aqueous solution (GO, 5mg/ml) was purchased from Titan. L-ascorbic acid, dioxane and 3-aminopropyltriethoxysilane (APTES) were obtained from Perimed. 1,3,5-Benzenetricarboxaldehyde (TFB) was purchased from Shanghai Aladdin Biochemical Technology. 5,5'-Diamino-2,2'-bipyridine (Bpy) was obtained from Jilin Zhongshen scientific research technology Co., Ltd. Hydrochloric acid (HCl; 36.0-38.0%) was bought from DaMao. KOH (85%) was acquired from Alfa Aesar. All the reagents were of analytical grade and were used as received.

### 1.2. Electrochemical measurements

#### 1.2.1 Electrocatalysis for OER and HER

All electrochemical measurements were performed at room temperature using a three-electrode system electrochemical workstation (Gamry Reference 600 Potentiostat). The working electrode, counter electrode, and reference electrode of the three electrode systems are rotating disk electrode (RDE), carbon rod and Ag/AgCl (4.0 M KCl), respectively. All measured potentials were converted to the reversible hydrogen electrode (RHE) according to the Nernst equation:

$$E_{RHE} = E_{Ag/AgCl} + 0.059pH + E_{Ag/AgCl}^0$$

Where  $E_{Ag/AgCl}$  is the measured potentials vs. Ag/AgCl,  $E_{Ag/AgCl}^0 = 0.1976$  V at 25 °C. The pH value of 0.1 M KOH was measured to be ~12.77. Thus, the  $E_{RHE}$  is calibrated as  $E_{RHE} = E_{Ag/AgCl} + 0.951$ .

Catalyst ink was obtained by ultrasonically dispersing 10 mg of catalyst in 1 ml of Nafion ethanol solution (5wt%) and stirring at room temperature for 24 h. Subsequently, 10  $\mu$ l of catalyst ink (10 mg mL<sup>-1</sup>) was pipetted onto the glassy carbon surface and dried at room temperature to form a uniform catalyst film. Polarization curves for the oxygen evolution reaction (OER) and hydrogen evolution reaction (HER) were measured in N<sub>2</sub>-saturated 0.1 M KOH electrolyte at a voltage of 1.0 ~ 2.0 V (vs RHE) and -1 ~ 0 V (vs RHE), respectively, with

a scan speed of  $5 \text{ mV s}^{-1}$  at 1600 r.p.m. For comparison, the commercial  $\text{RuO}_2$  and Pt/C catalysts were measured under identical conditions for OER and HER, respectively. All polarization curves were corrected with IR-compensation.

The electrochemical impedance spectroscopy (EIS) of HER and OER were carried out in an  $\text{N}_2$ -saturated 0.1 M KOH electrolyte from 10 kHz to 0.01 Hz with a 5 mV AC potential at 1600 r.p.m. The stability tests for the GA@Bpy-COF-Co were conducted using chronopotentiometry at a current density of  $10 \text{ mA cm}^{-2}$ .

### 1.2.2 Overall water splitting

Overall water splitting was performed in a two-electrode cell using self-standing GA@Bpy-COF-Co as both anode and cathode electrodes. To prepare the self-standing electrode, a graphitic nanorods ( $D = 2 \text{ mm}$ ) was applied to insert into GA during its fabrication process. Then the electrode was immersed in cobalt acetate ( $\text{Co}(\text{OAc})_2 \cdot 4\text{H}_2\text{O}$ ) solutions in methanol and further stirring for 4 h at RT for Co incorporation. The modified electrode was dried in a vacuum oven at  $60 \text{ }^\circ\text{C}$  for 30 min. Before measuring, the electrodes were first moistened by dipping in a mixture of ethanal and water (50:50 v/v), then multiple times in electrolyte.

### 1.2.3 Electrochemical surface area (ECSA)

Electrochemical active surface area (ECSA) was estimated by measuring the capacitance of the double layer at the solid-liquid interface with cyclic voltammetry (CV). The measurement was performed among a potential window of 0.55-0.65 V vs RHE, where the Faradic current on working electrode is negligible. The series of scan rates ranging from 40 to  $120 \text{ mV s}^{-1}$  were applied to build a plot of the charging current density differences against the scan rate at a fixed potential 0.60 V. The slope of the obtained linear is twice of the double-layer capacitance  $C_{dl}$ . ECSA was estimated by the equation:  $\text{ECSA} = C_{dl}/C_s$ , where the specific capacitance value ( $C_s$ ) was taken  $0.04 \text{ mF cm}^{-2}$ . The ECSA-normalized LSV curves were acquired by the equation:  $j_{\text{ECSA}} = i/\text{ECSA}$ , where  $j_{\text{ECSA}}$  and  $i$  is the current density normalized to ECSA and current of the working electrode, respectively.

### 1.2.4 Turnover frequency (TOF)

The turnover frequency (TOF) was evaluated by the following standard equation:

$$\text{TOF} = (j \times A) / (4 \times F \times n)$$

Where  $j$  (A/cm<sup>2</sup>) is the current density at a given overpotential,  $A$  is the geometric surface area of the electrode,  $F$  stands for the Faraday constant,  $n$  (mol) is molar amount of cobalt loaded on the GC electrode which was determined by the ICP-OES analysis. All metal cations in the COFs were assumed to be catalytically active, so the calculated value represents the lower limits of the TOF.

### 1.2.5 Faradaic efficiency

The Faradaic efficiency was calculated by comparing the experimentally produced gas volume with the theoretically calculated one:

$$\eta_{\text{Faraday}} = V_{\text{experimental}}/V_{\text{theoretical}}$$

The experiment volume of H<sub>2</sub> and O<sub>2</sub> can be obtained from experimental data. The theoretical volume can be calculated using the formula:

$$V_{\text{theoretical}} = I \cdot t \cdot V_m / n \cdot F$$

where  $I$  is the current measured in the experiment,  $t$  is the measured time,  $V_m$  is the molar volume of H<sub>2</sub> or O<sub>2</sub> in l/mol,  $n$  is the number of electrons required for one molecule H<sub>2</sub> or O<sub>2</sub> and  $F$  is the Faraday constant (96485 C/mol).

### 1.3. Characterization

PXRD patterns were measured on a Bruker D8 Advance instrument with Cu K $\alpha$  radiation ( $\lambda=1.54$  Å) at a generator voltage of 40 kV and a generator current of 40 mA with a scanning speed of 2 °/min from 2° to 60°. FT-IR spectra were performed on a Thermo Scientific Nicolet iS5. Nitrogen sorption measurements were carried out on a Quantachrome Quadrasorb SI instrument. All samples were degassed at 120 °C for 12 h before actual measurement. The surface area was calculated by using Brunauer-Emmett-Teller (BET) calculations and the pore size distribution plot was obtained from the adsorption branch of isotherms by the QSDFT model. SEM measurements were conducted on Hitachi S4800. TEM images were obtained from FEI Tecnai F20. The samples for TEM analyses were prepared by dispersing the electrocatalysts in ethanol, followed by dropping it onto a copper grid covered with carbon film. XPS spectra were performed on a Thermo Scientific K-Alpha.

## **Section 2. Experiment section**

### **2.1 Preparation of GA<sup>s1</sup>**

In a typical synthesis, Graphene oxide (GO, 3mg/ml, 5ml) and L-ascorbic acid (45mg) were added to a 10 mL sample bottle. The mixture was stirred for 10 min to get a homogenous dispersion. Subsequently, the bottle was placed in an ordinary oven at 95 °C and left undisturbed for 5 h to form a reduced hydrogel. The hydrogel was soaked in 5:1 alcohol aqueous solution for 2 days. Finally, the hydrogel was freeze-dried for 24 hours by a freeze dryer to obtain graphene aerogel (GA).

### **2.2 Preparation of GA-NH<sub>2</sub>**

First, GA was added to the concentrated hydrochloric acid solution (10ml) and heated at 60 °C in an oil bath for 4 h, followed by washing with distilled water and freeze-dried for 10 h. Then, GA was added to 7.5 mL of methylbenzene by sonication for 1 min before adding 3-aminopropyltriethoxysilane (APTES, 93mg). Then, the mixture was stirred at 30 °C and 100 °C for 3 h in N<sub>2</sub> atmosphere, respectively. Upon cooling to room temperature, the residue was washed with methylbenzene, ethanol and pure water and freeze-dried for 10 h to get the GA-NH<sub>2</sub>.

### **2.3 Preparation of GA@Bpy-COF**

GA-NH<sub>2</sub> and 10 mg of 1,3,5-Benzenetricarboxaldehyde (TFB) were mixed in 10 mL of dioxane. The mixture was sonicated for 2 min, then heated at 150 °C for 1 h to obtain COF with aldehyde group modification. When cooled to room temperature, the products were immersed in 10 ml of dioxane with 16 mg of 5,5'-Diamino-2,2'-bipyridine (Bpy), 10 mg of TFB, and 200 μL of acetic acid (6M). Then, a step-growth polymerization approach was conducted through standing growth at room temperature (RT) for 24 h and solvothermal treatment at 120 °C for 48 h, respectively. The product was sequentially washed with dioxane and acetone, and freeze-dried 10 h to get the GA@Bpy-COF.

### **2.4 Preparation of GA@Bpy-COF-Co**

GA@Bpy-COF-Co was prepared by soaking a defined amount of GA@Bpy-COF in

methanolic cobalt acetate solution and stirring for 4 h. Then the sample was washed with a large amount of dry methanol. The obtained GA@Bpy-COF-Co was finally obtained after drying overnight in a vacuum oven at 60 °C. Other transition metal salts [Fe(OAc)<sub>2</sub>, Ni(OAc)<sub>2</sub>·4H<sub>2</sub>O, Cu(OAc)<sub>2</sub>, Zn(OAc)<sub>2</sub>·2H<sub>2</sub>O, Mn(OAc)<sub>2</sub>·4H<sub>2</sub>O] were used for the corresponding GA@Bpy-COF-M preparation with the similar procedure.

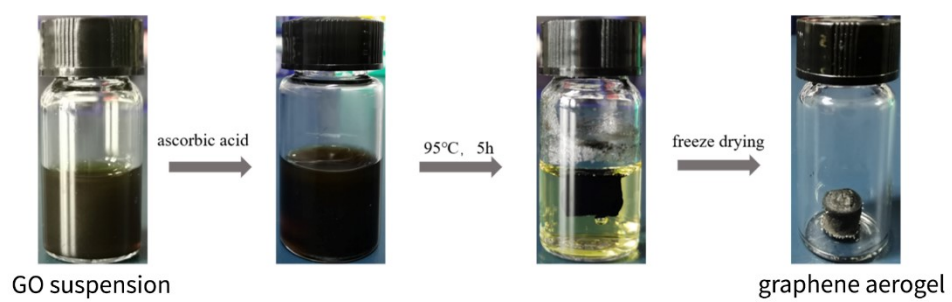


Fig. S1. Synthetic procedure for GA preparation.

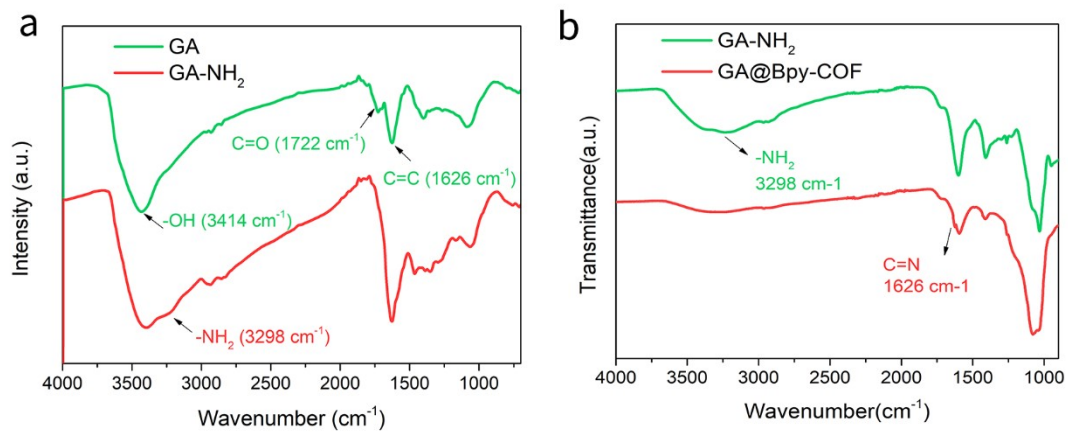


Fig. S2. FT-IR spectra of GA, GA-NH<sub>2</sub>, and GA@Bpy-COF.

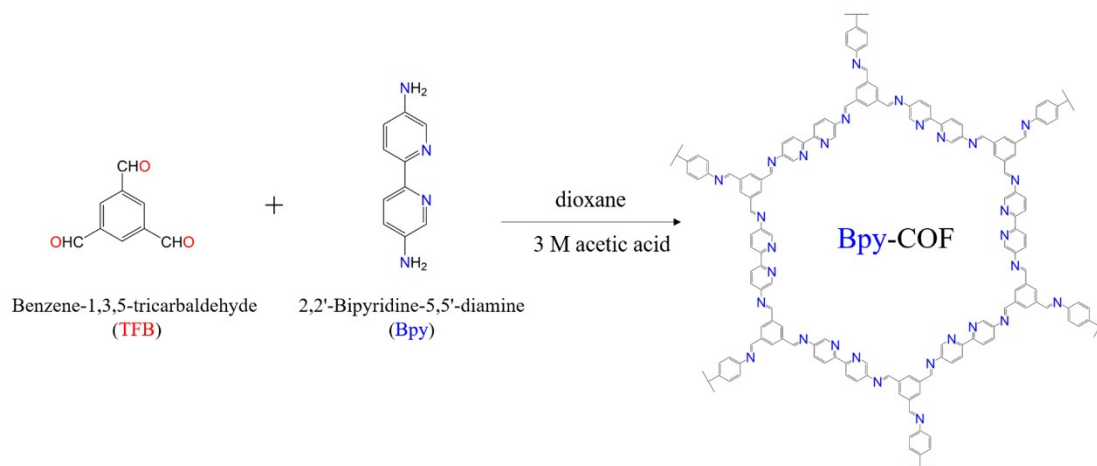


Fig. S3. Structure and synthetic procedure for Bpy-COF via Schiff-based polymerization.

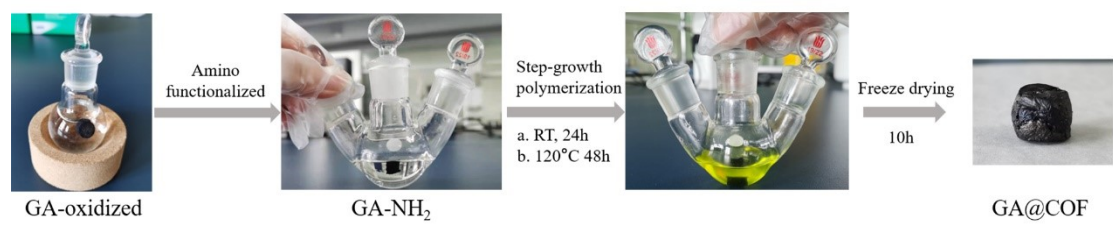


Fig. S4. The step-growth polymerization for GA@COF preparation.

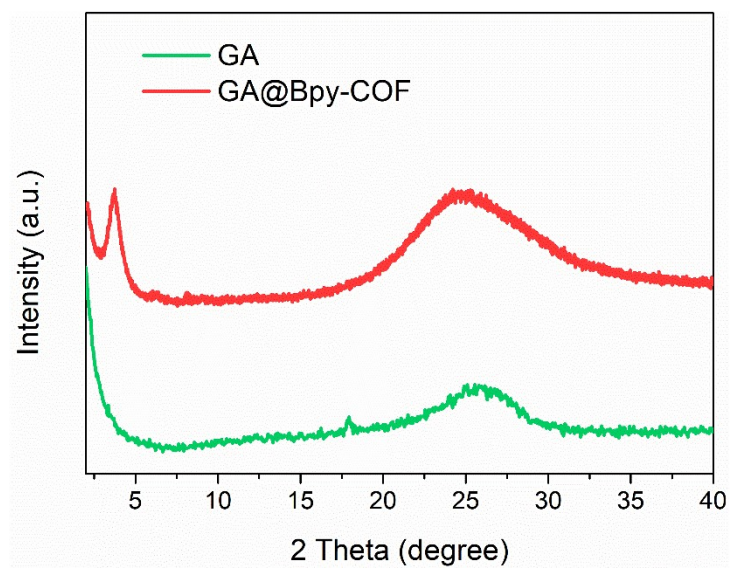


Fig. S5. PXRD patterns of GA and GA@Bpy-COF.

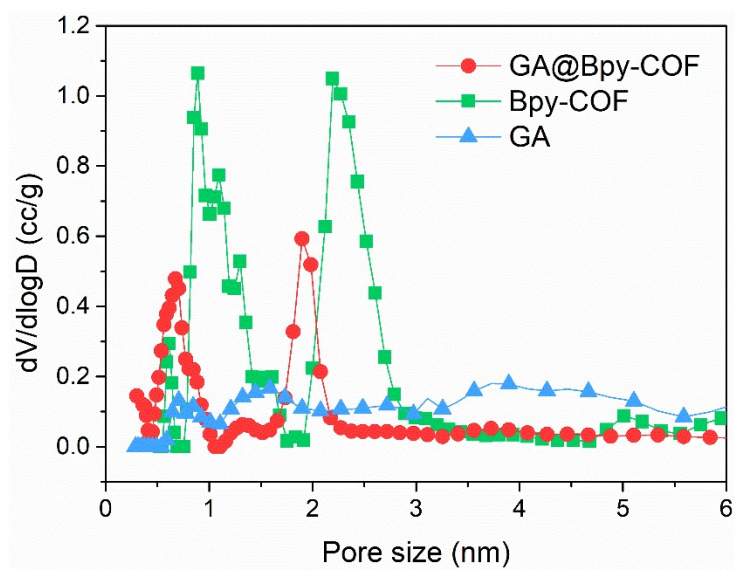


Fig. S6. Pore size distribution of the GA@Bpy-COF-Co, Bpy-COF and GA.

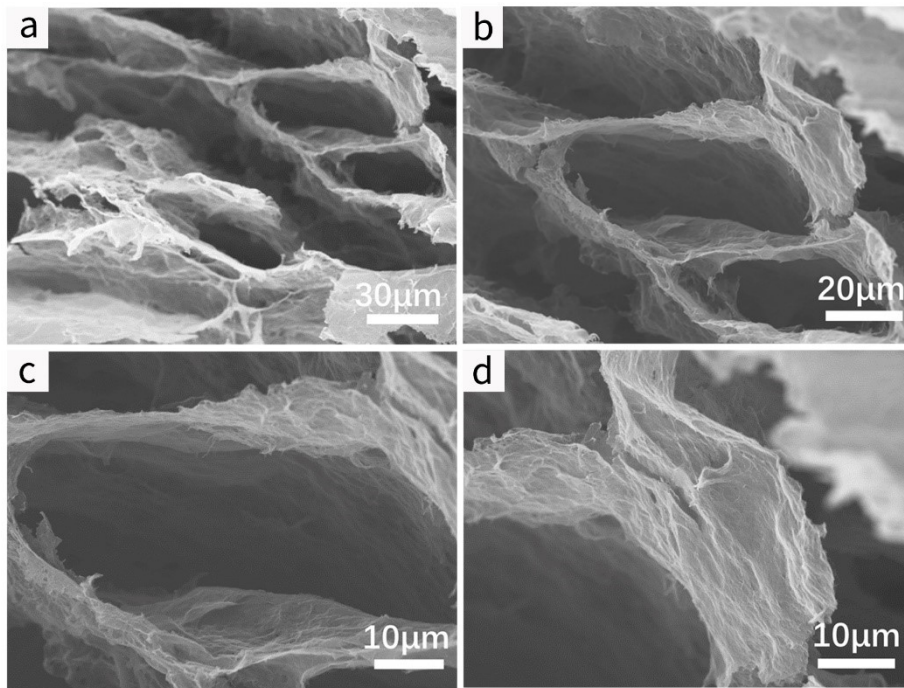


Fig. S7. SEM images of as-synthesized GA.

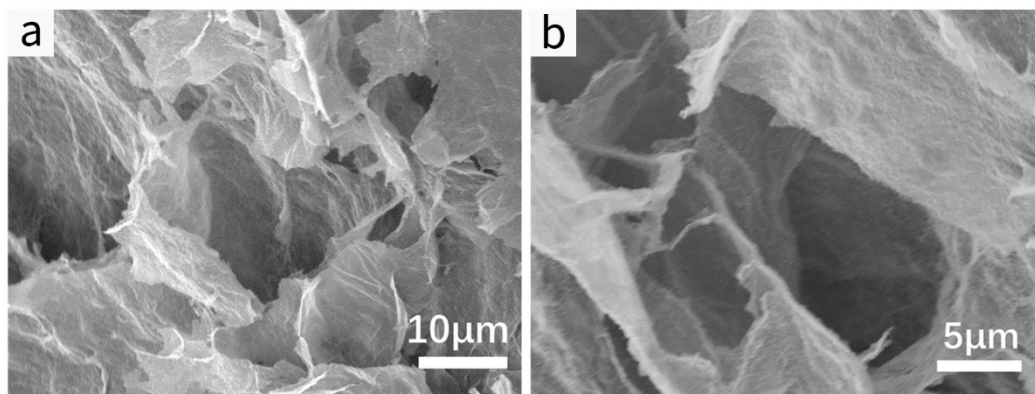


Fig. S8. SEM images of GA@Bpy-COF.

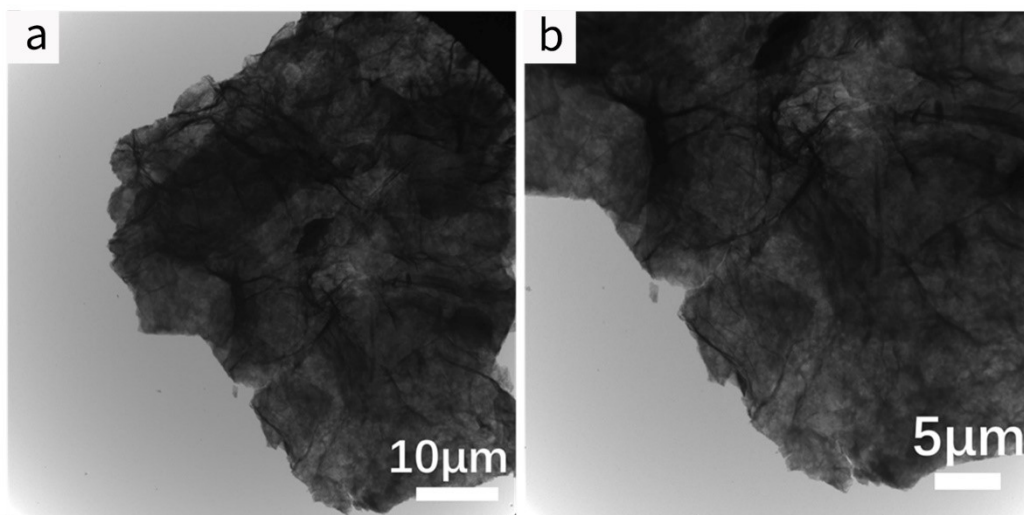


Fig. S9. TEM images of GA@Bpy-COF.

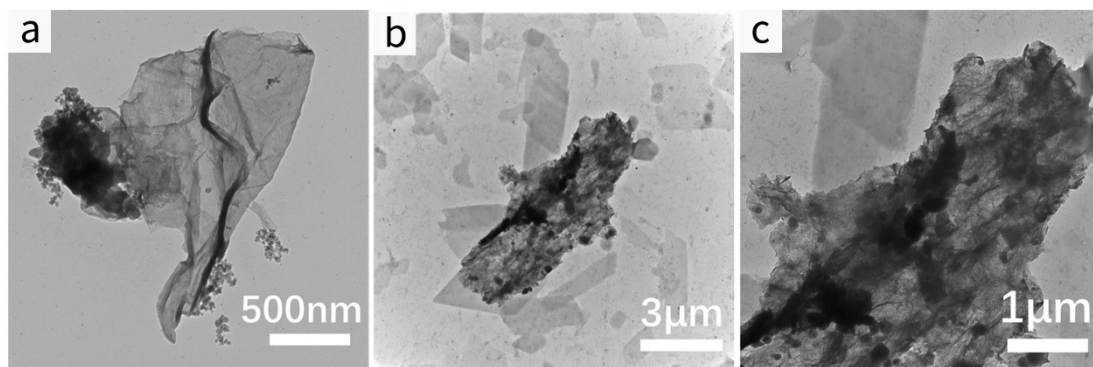


Fig. S10. TEM images of GA without amino functionalization for COF growth.

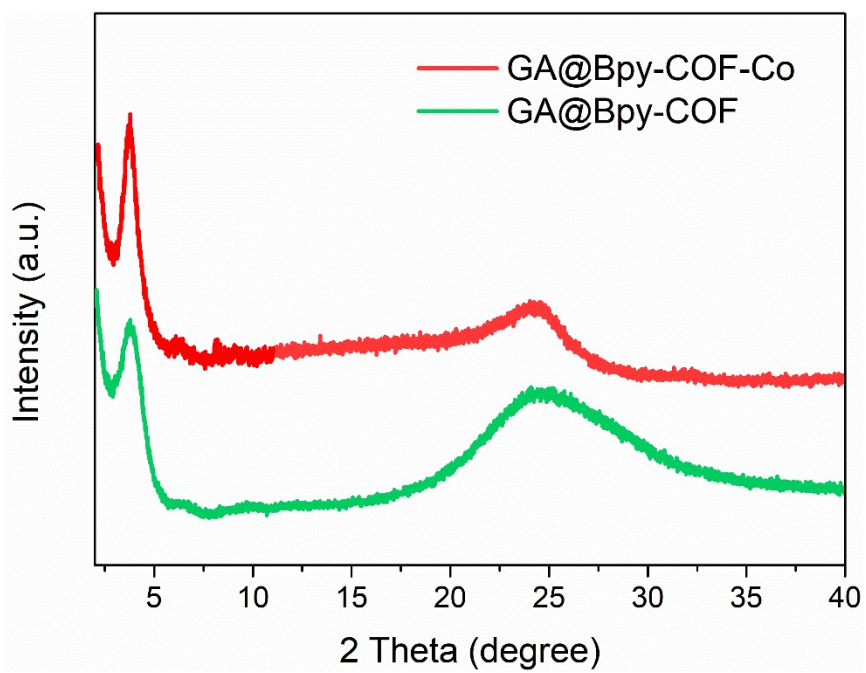


Fig. S11. PXRD patterns of GA@Bpy-COF-Co and GA@Bpy-COF.

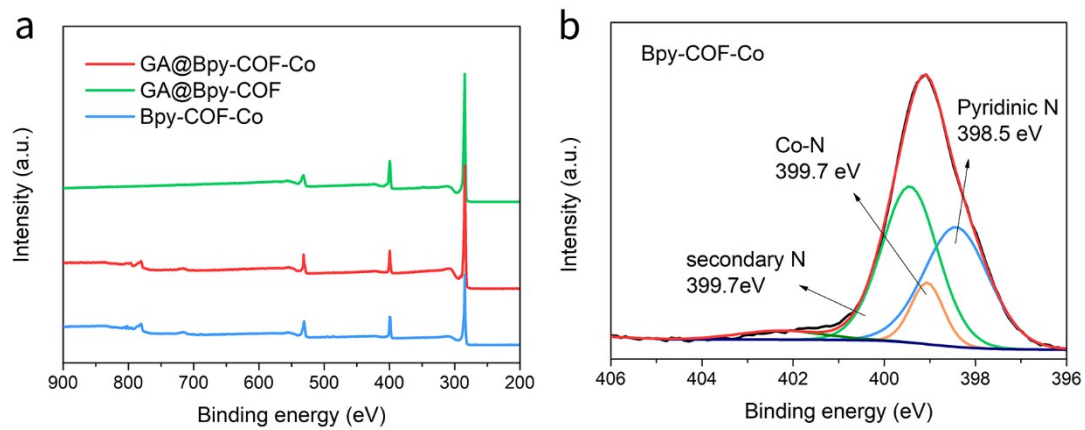


Fig. S12. a) XPS survey scan of the GA@Bpy-COF-Co, GA@Bpy-COF and Bpy-COF-Co. b) High resolution N1s spectra of Bpy-COF-Co.

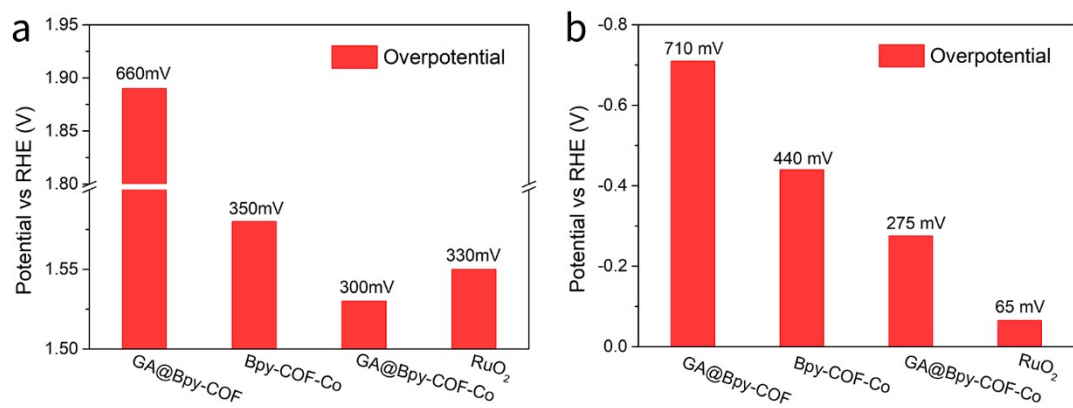


Fig. S13. Overpotential of GA@Bpy-COF-Co for a) OER and b) HER, respectively, at a current density of 10 mA cm<sup>-2</sup>.

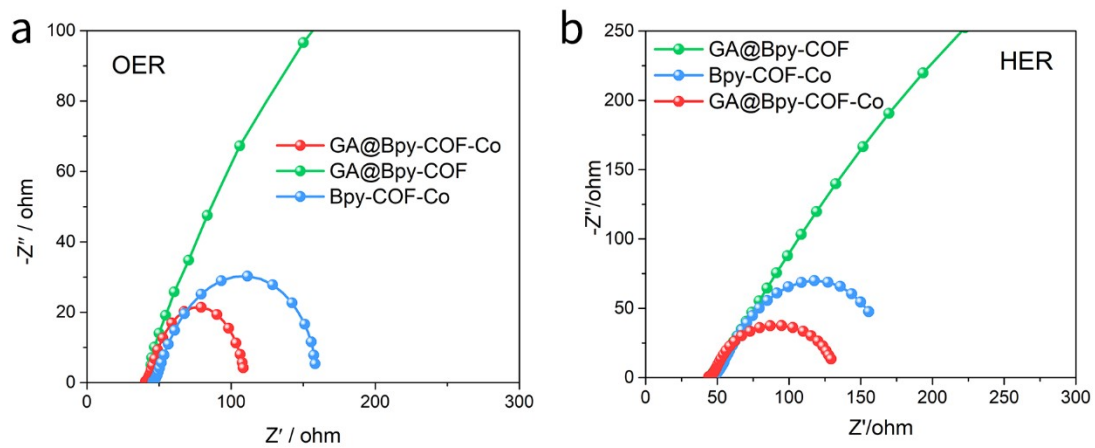


Fig. S14. EIS spectra of the GA@Bpy-COF-Co, GA@Bpy-COF, and Bpy-COF-Co recorded at a constant potential of 1.530 V and -0.275 V (vs. RHE) for OER and HER, respectively.

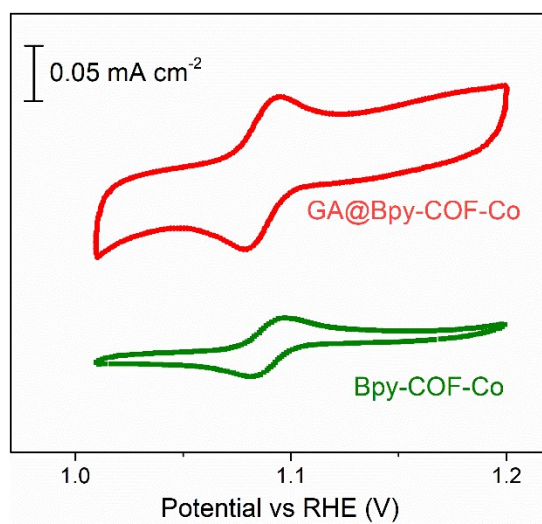


Fig. S15. CV of GA@Bpy-COF-Co and Bpy-COF-Co.

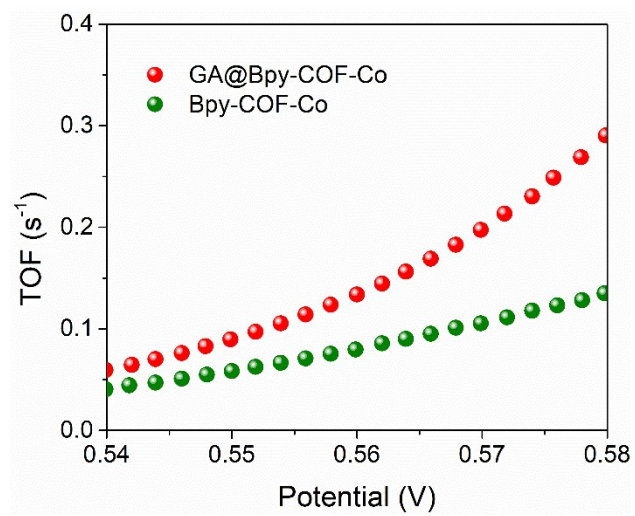


Fig. S16. TOF plots of GA@Bpy-COF-Co and Bpy-COF-Co during the OER.

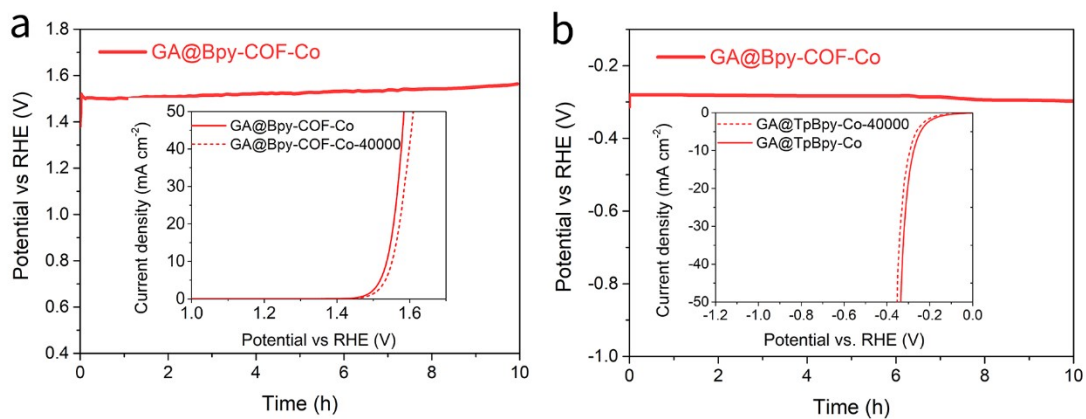


Fig. S17. a) Chronopotentiometry test of GA@Bpy-COF-Co catalysts at a constant current density of 10 mA cm<sup>-2</sup> in a) OER process. Inset: OER polarization plots of GA@Bpy-COF-Co before and after 40 000 s. b) HER process. Inset: HER polarization plots of GA@Bpy-COF-Co before and after 40 000 s.

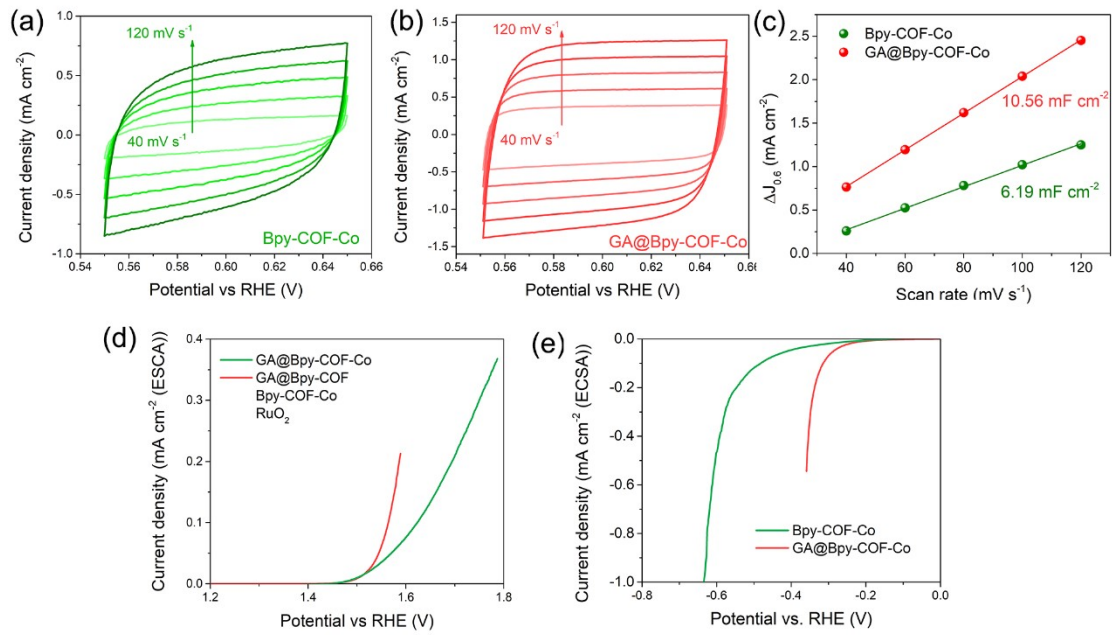


Fig. S18. CVs of (a) Bpy-COF-Co and (b) GA@Bpy-COF-Co in 0.1 M KOH at different scan rates from 40, 60, 80, 100 and 120 mV s<sup>-1</sup>. (c) Electrochemical double-layer capacitance. ECSA-normalized LSV curves of Bpy-COF-Co and GA@Bpy-COF-Co for (d) OER and (e) HER.

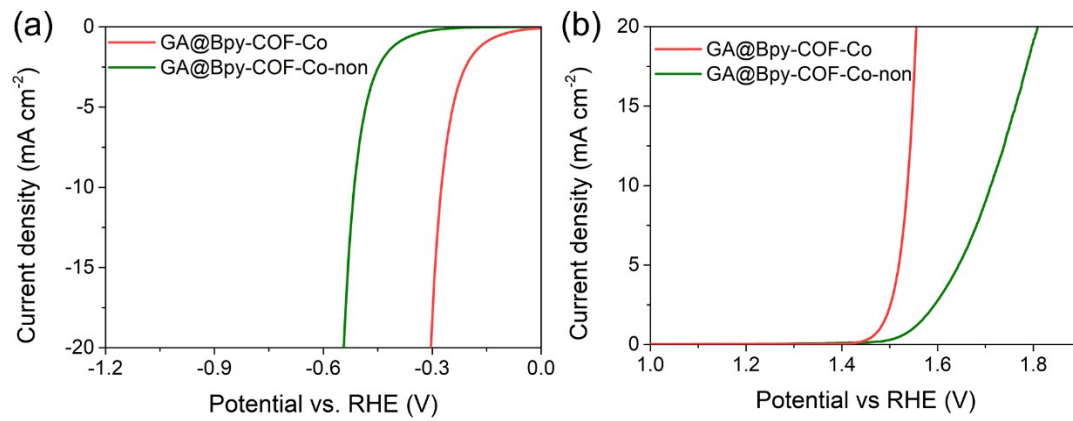


Fig. S19. (a) HER (b) OER performances of GA@Bpy-COF-Co and GA@Bpy-COF-Co-non.

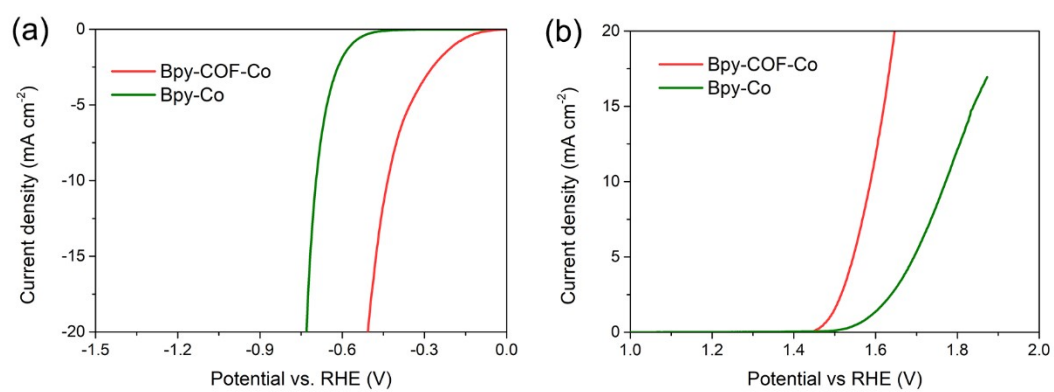


Fig. S20. (a) HER (b) OER performances of Bpy-COF-Co and Bpy-Co.

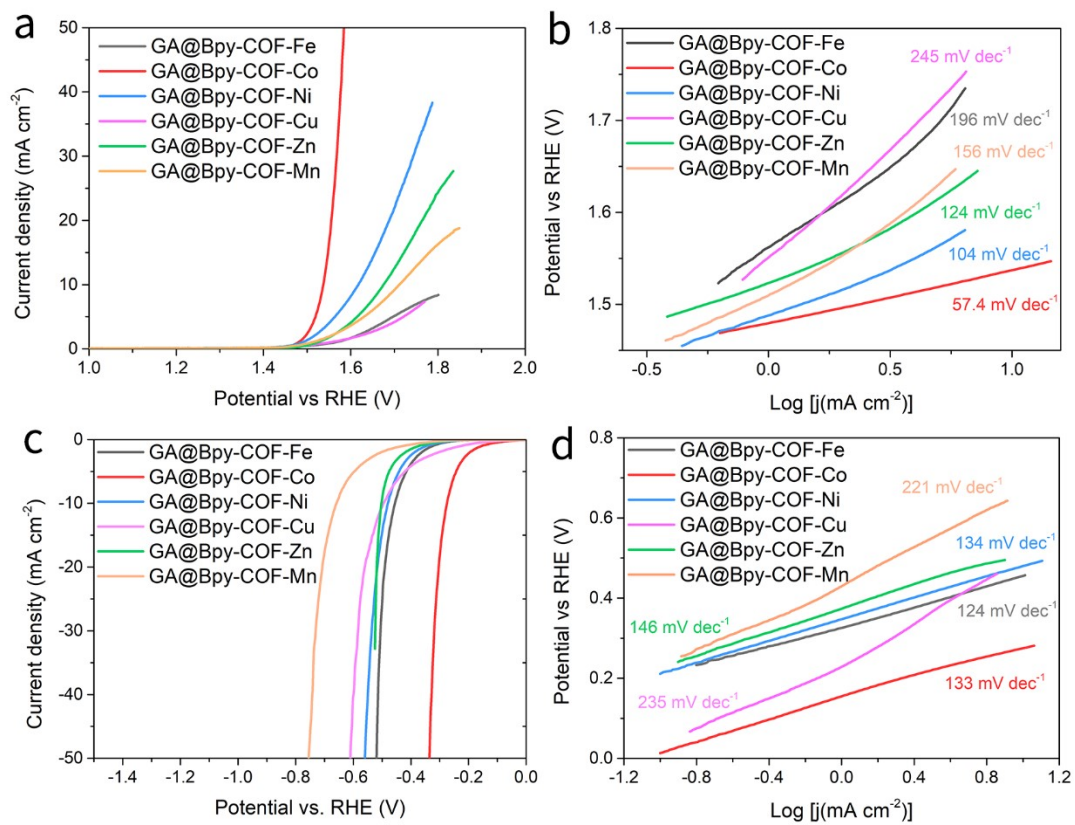


Fig. S21. a) OER polarization curves, b) Corresponding Tafel slopes for GA@Bpy-COF-M with various metal ions. c) HER polarization curves, d) Corresponding Tafel slopes for GA@Bpy-COF-M with various metal ions.

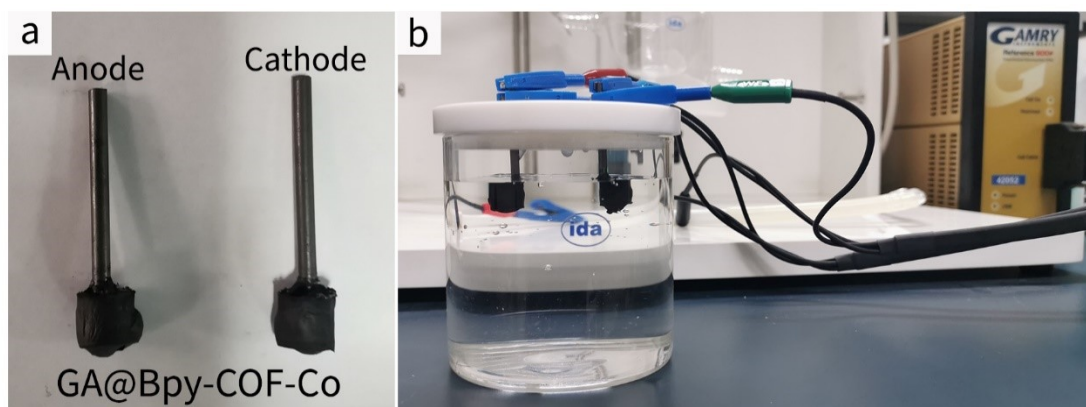


Fig. S22. Photographs of a) GA@Bpy-COF-Co electrodes. b) working electrolyzer in 1.0 M KOH solution.

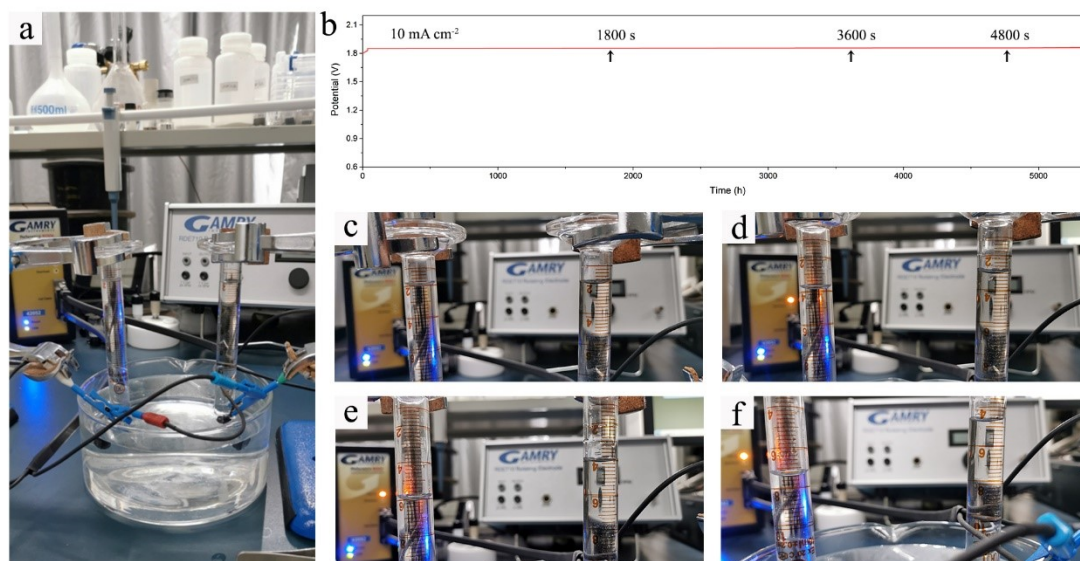


Fig. S23 a) Photograph of lab-made gas collector for  $\text{H}_2$  and  $\text{O}_2$  production. b) Chronopotentiometry of GA@Bpy-COF-Co electrocatalyst, and photographs of lab-made gas collectors at the time of : c) 0s, d) 1800s, e) 3600s, and f) 4800s.

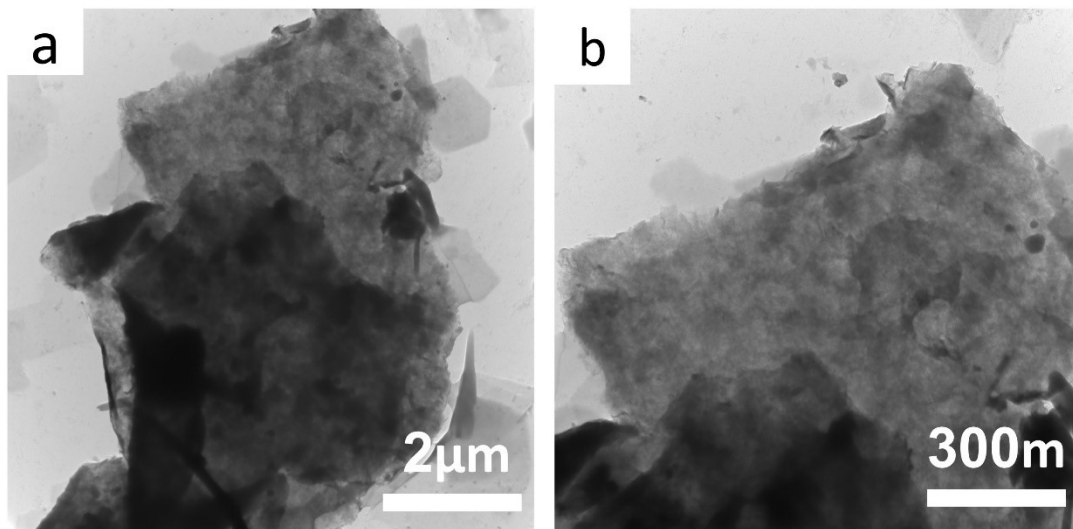


Fig. S24. TEM images of GA@Bpy-COF-Co-10h.

Table S1 Summary of recently reported OER and HER performances of other reported transition metal-based electrocatalysts under alkaline condition.

	Catalyst	$\eta_{10}$ (mV) for OER	Tafel slope (mV dec <sup>-1</sup> ) for OER	$\eta_{10}$ (mV) for HER	Tafel slope (mV dec <sup>-1</sup> ) for HER	electrolyte	Reference
0	<b>GA@Bpy-COF-Co</b>	<b>300</b>	<b>54</b>	<b>275</b>	<b>139</b>	<b>0.1 M</b>	<b>Our work</b>
	GA@Bpy-COF	660	259	710	170	<b>KOH</b>	
	Bpy-COF-Co	350	85	440	169		
1	Fe-Co <sub>1.11</sub> Te <sub>2</sub> @NCNTF	297	91	107	73	1.0M	<i>ChemSusChem</i> <b>2020</b> , 13, 5239-5247.
	Co <sub>1.11</sub> Te <sub>2</sub> @NCNTF	360	181	185	180	KOH	
2	Fe-Ni@NC-CNTs	274	45.47	202	113.7	1.0M	<i>Int Ed Engl</i> <b>2018</b> , 57, 8921-8926.
	Fe-Ni@C	470	178.6	356	196.3		
	Fe-Ni@NC-powder	370	56.44	409	175.4	KOH	
3	CuCoSe@HCNF	260 (j=20mA cm <sup>-2</sup> )	57	181	59	1.0M KOH	<i>Appl. Catal. B: Environ.</i> <b>2021</b> , 293, 120209.
	CuCoSe	320 (j=20mA cm <sup>-2</sup> )	76	234	67		
4	Co@IC/MoC@PC	282 (0.1M KOH)	82	68	87	1.0M	<i>ACS Nano</i> <b>2021</b> , 15, 13399-13414.
	Co@IC	356 (0.1M KOH)	99	233	146	KOH	
	Co@IC@PC	380 (0.1M KOH)	101	248	158		
5	Co/CoP@HOMC	260	151	120	78	1.0M	<i>Adv Energy Mater</i> <b>2021</b> , 11, 2102134.
	CoP@HOMC	290	159	150	95		
	Co@HOMC	340	217	160	253	KOH	
	Co/CoP@NC	310	176	210	98		
6	NiCoOS	470	/	300	/	0.1M KOH	<i>Nano Energy</i> <b>2019</b> , 58, 680-686.
7	Ni <sub>0.85</sub> Se@NC	300	125	157	153	1.0M	<i>CCS Chemistry</i> <b>2021</b> , 3, 2696-2711.
	NiSe <sub>2</sub> @NC	340	153	210	216	KOH	
8	CoFeN-NCNTs//CCM	325	49	151	130	1.0M	<i>Adv. Funct. Mater.</i> <b>2021</b> , 32, 2107608.
	Co-NCNTs//CCM	407	131	304	143		
	FeC-NCNTs//CCM	431	105	351	138	KOH	
	CoFeN-CCM	363	60	282	134		
9	FeTPP@NiTPP/NF	302(j=100mA cm <sup>-2</sup> )	110.0	170	172.4	1.0M KOH	<i>Int J Hydrogen Energy</i> 2020, 45, 28860-28869.
	NiTPP/NF	451(j=100mA cm <sup>-2</sup> )	125	212	181.1		
	TPP/NF	491(j=100mA cm <sup>-2</sup> )	256	225	329.4		
	ZIF-67	427	130.52	425	110.95		

9	ZIF-67@PBA	288	80.07	376	102.36	1.0M KOH	<i>Chem Eng J</i> <b>2021</b> , 403, 126312.
	CoP/NC	276	74.33	213	70.33		
	CoP@FeCoP/NC	238	47.98	141	56.34		
10	C-CoP-1/12	333	71.1	173	63.1	1.0M	<i>Nanoscale</i> <b>2019</b> , 11, 17084-17092.
	C-Co <sub>3</sub> O <sub>4</sub>	424	93.4	577	166.4	KOH	
11	Cu <sub>0.3</sub> Co <sub>2.7</sub> P/NC	190	57	220	122	1.0M KOH	<i>Adv Energy Mater</i> <b>2017</b> , 7, 1601555.
12	Co <sub>2</sub> B-500	380	45	328	177	1.0M KOH	<i>Adv. Energy. Mater.</i> <b>2016</b> , 6, 1502313.
13	NFN-MOF/NF	240	58.8	87	35.2	1.0M KOH	<i>Adv Energy Mater</i> <b>2018</b> , 8, 1801065.
14	CS-NFO@PNC-700	217	66	200	130	1.0M KOH	<i>Appl Catal B-Environ</i> <b>2022</b> , 300, 120752.
15	Co <sub>6</sub> W <sub>6</sub> C@NC/CC	286	53.96	59	45.39	1.0M KOH	<i>Small</i> <b>2020</b> , 16, 1907556.
	W <sub>2</sub> C@NC/CC	368	58.54	147	53.80		
	Co/CC	387	63.28	300	97.25		
16	Co@NPC	360	53	325	117	1.0M NaOH	<i>Nanoscale Adv</i> <b>2019</b> , 1, 2293-2302.
17	CC-NC-NiFeP	145	47	94	70	1.0M KOH	<i>Nanoscale</i> <b>2020</b> , 12, 8443-8452.
18	NiFe-MS/MOF@NF	230	32	90	82	1.0M	<i>Adv Sci</i> <b>2020</b> , 7, 2001965.
	NiFe-MOF@NF	281	64	170	98	KOH	
19	FeNiP/PG	229	49.7	173	50.3	1.0M KOH	<i>J Mater Chem A</i> <b>2019</b> , 7, 14526-14535.
	FeNiP/GC/PG	239	49.7	298	98.7		
	FeNiP/RGO	246	80.5	187	85.1		
20	Co-Ni-Se/C/NF	275 (j=30mA cm <sup>-2</sup> )	63	90	81	1.0M KOH	<i>J Mater Chem A</i> <b>2016</b> , 4, 15148-15155.
	NiCo LDH/C/NF	270 (j=20mA cm <sup>-2</sup> )	110	148	122		
21	Ni <sub>2</sub> (dobpdc)	288	114	176	87	1.0M KOH	<i>J Mater Chem A</i> <b>2020</b> , 8, 22974-22982.
	Fe <sub>2</sub> (dobpdc)	233	48	152	83		
	NiFe(dobpdc)	207	36	113	69		
22	Ni <sub>2</sub> P/rGO	260	62	142	58	1.0M KOH	<i>J Mater Chem A</i> <b>2018</b> , 6, 1682-1691.
	Ni <sub>2</sub> P/C	275	88	185	75		
	Ni <sub>2</sub> P	355	107	310	104		

Table S2 Faradaic efficiency of the produced hydrogen and oxygen amount during the water-splitting process

Time/s	H <sub>2</sub>			O <sub>2</sub>		
	V <sub>experimental</sub> /ml	V <sub>theoretical</sub> / ml	η <sub>Faraday</sub> /%	V <sub>experimental</sub> /ml	V <sub>theoretical</sub> / ml	η <sub>Faraday</sub> /%
0	0	0	0	0	0	0
600	0.65	0.6964	93.33	0.32	0.3482	91.90
1200	1.35	1.3929	96.92	0.65	0.6964	93.34
1800	1.95	2.0894	93.32	1	1.0447	95.72
2400	2.75	2.7859	98.71	1.36	1.3929	97.64
3000	3.41	3.4824	97.92	1.7	1.7412	97.63
3600	4.05	4.1788	96.92	2.05	2.0894	98.11
4200	4.8	4.8753	98.46	2.4	2.4376	98.46
4800	5.4	5.5718	96.91	2.7	2.7859	96.92

## References

[s1] Huang, X.; Yu, G.; Zhang, Y.; Zhang, M.; Shao, G. Design of cellular structure of graphene aerogels for electromagnetic wave absorption. *Chem. Eng. J.*, **2021**, *426*, 131894.